

# Spatiotemporal chaos in the parametric excitation of a capillary ripple

A. B. Ezerskiĭ, M. I. Rabinovich, V. P. Reutov, and I. M. Starobinets

*Institute of Applied Physics, Academy of Sciences of the USSR*

(Submitted 2 May 1986)

Zh. Eksp. Teor. Fiz. **91**, 2070–2083 (December 1986)

The development of turbulence on the surface of a liquid when it is parametrically excited is investigated experimentally and theoretically. It is shown that modulation in the form of quasiperiodic “focusing” appears with increase of the supercriticality  $\varepsilon$  on the background of the Faraday ripple, and with further increase of  $\varepsilon$  this focusing goes over (via intermittency) into spatiotemporal chaos. The dynamical nature of the observed chaos is established and a theory that gives a satisfactory description of the observed phenomena is constructed.

## 1. INTRODUCTION

The problem of the parametric generation of waves by a uniform oscillating field is interesting for many areas of physics—the generation of Langmuir waves in a plasma, of spin waves in ferromagnets, and of waves on the surface of a dropping liquid, a liquid dielectric in an electric field, or a ferromagnetic liquid in an alternating magnetic field.<sup>1–4</sup> One unexpected manifestation of the parametric instability is the appearance of wave formations on the surface of a molten metal heated by modulated ion beams.<sup>5</sup>

The parametric excitation of surface waves on water in a varying gravitational-force field was investigated long ago and is the most visualizable of the phenomena mentioned (the first observation was made by Faraday in 1831). On this subject there is now a large number of theoretical papers, which are mainly devoted to determining the threshold for generation and to finding the amplitudes of the stationary standing waves in different approximations.<sup>6</sup> It is obvious that such a formulation of the problem is justified only for parametric excitation of not-too-high modes of a high- $Q$  resonator. In a sufficiently long system spatially nonuniform nonstationary distributions of wave fields should be observed. Such distributions and the onset of capillary-wave turbulence have been detected on the surface of silicone.<sup>7</sup> Below, this phenomenon is investigated in detail, and a theory of it is constructed.

We draw attention to the fact that the capillary-ripple parametric turbulence investigated here is not described by the familiar  $S$ -theory of Ref. 2, since even for extremely large supercriticalities, when the capillary ripple is already “random,” the spatial spectra in the experiments are not continuous but have the form of a set of smeared peaks. Thus, in the experiments a situation is realized in which it is necessary to describe the development of spatiotemporal chaos in the ensemble of capillary waves in the framework of a purely dynamical model, without *a priori* hypotheses concerning, say, the absence of correlation of the phases of pairs of parametrically excited waves. For this, in the present paper, we use parabolic equations for the plane capillary waves.

## 2. EXPERIMENT

A description of the apparatus and the results of the first series of experiments are given in Ref. 7. In this series of experiments we used silicone with the following parameters: density  $\rho = 0.9$  g/cm<sup>3</sup>, surface-tension coefficient  $\alpha = 23$  dyne/cm, and kinematic-viscosity coefficient  $\nu = 0.04$  cm<sup>2</sup>/sec. A capillary ripple was excited on the surface of a thin layer (of thickness  $\sim 10$  mm) of the oil, deposited onto a vibrating metal plate. The boundary of the layer was a ring with inner diameter 18 cm. At a pumping frequency  $\sim 140$  Hz capillary waves with frequency  $f \cong 70$  Hz were excited. Here the wavelength was  $\lambda \cong 3.2$  mm, and this guaranteed fulfillment of the deep-water condition.

Allowance for the vibrations of the liquid layer can reduce to the introduction of an oscillatory correction to the acceleration of free fall. When the amplitude  $G$  of this correction exceeded a certain threshold value  $G_c$  ( $G_c \cong 4.2g$  at the pumping frequency 140 Hz), there appeared in the center of the cuvette<sup>1)</sup> a Faraday ripple which, in the reflected light of the pumping lamp, gave an image in the form of a network with square cells. The calculations give good agreement of the threshold  $G_c$  with the results of theory for the spatially uniform excitation of a standing wave (Ref. 8).<sup>2)</sup> For supercriticalities  $\varepsilon = G/G_c - 1 \cong 0.2$  the Faraday ripple filled the whole surface of the layer. However, even for  $\varepsilon < 0.2$  modulation appeared in the contrast of the image of the primary cell structure, in the form of bands stretched along the principal axes of the network (Fig. 1). With strong illumination of the surface, the principal observed features were troughs (dark bands) in the distribution of the contrast.<sup>7</sup> The system of dark bands was in continuous motion, which became faster and more complicated with increase of the supercriticality. Thus, we observed displacement of the bands, parallel to themselves and with unchanged orientation, mainly through distances of the order of the size of a band, changes of brightness, the creation and disappearance of troughs, and also rotations, discontinuities, etc. At low supercriticalities the almost one-dimensional modulation along one of the principal directions of the network could be replaced spontaneously, after a time of the order of 10 sec, by

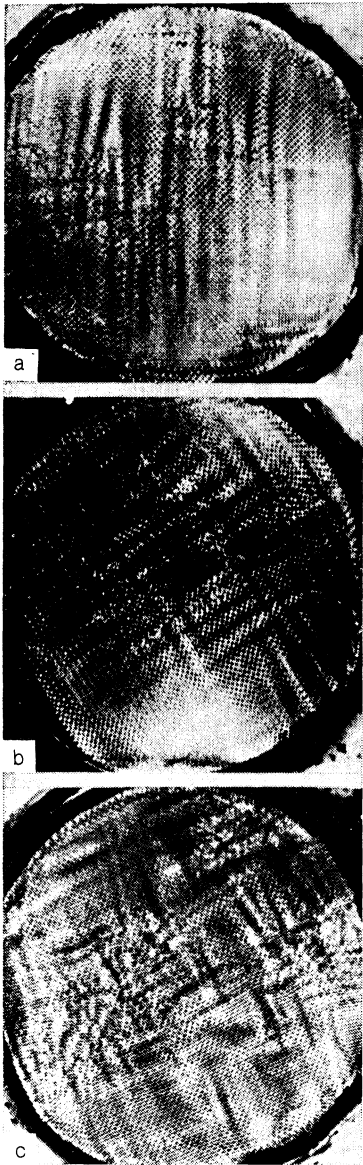


FIG. 1. Structures of the capillary ripple on the surface of a vibrating layer of silicone upon increase of the supercriticality  $\varepsilon$ : a)  $\varepsilon = 0.4$ ; b)  $\varepsilon = 0.53$ ; c)  $\varepsilon = 1.13$ .

modulation along another direction. By visual estimation, the characteristic times of the enumerated changes in the system of bands decreased from values  $\sim 1$  sec at low supercriticalities to tenths of a second at  $\varepsilon \cong 1$ . With increase of the supercriticality the spatial pattern of the modulation became more and more two-dimensional and disordered; see Fig. 1c. For  $\varepsilon \cong 1.7$  drops began to break away from the surface of the layer.

As is well known, the appearance of a Faraday ripple is due to the parametric generation of pairs of oppositely moving waves. In the case of excitation of two wave pairs with orthogonal fronts the cells of the surface relief have the form of squares. It is natural to postulate that the observed modulation of the image contrast is due to spatiotemporal modulation of the amplitudes of the parametrically excited waves.<sup>3)</sup>

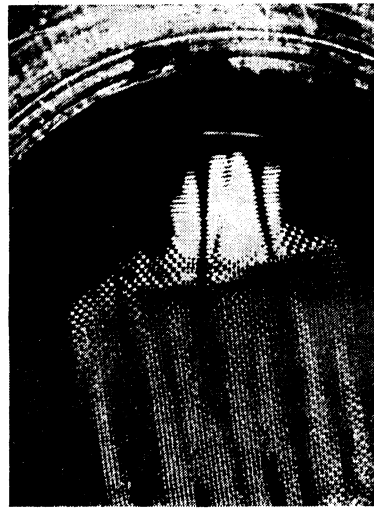


FIG. 2. Transverse modulation of a standing ripple wave outside the region with square cells (supercriticality  $\varepsilon = 0.1$ ).

Analysis of the periods of the modulation suggests that for the complex amplitude  $a$  of the waves the conditions for smooth variation in space are fulfilled:

$$|ka^{-1}\partial a/\partial x| \ll 1, \quad |ka^{-1}\partial a/\partial y| \ll 1, \quad (1)$$

where  $x$  and  $y$  are the directions of propagation of the wave pairs, and  $k$  is the wave number. In particular, for a typical modulation with period  $3\lambda$  the left-hand side in (1) is  $\sim 0.33$ . The narrowness (used here) of the spatial spectra of the wave packets is confirmed by the results of an optical spectral analysis of images of the surface.<sup>7</sup> The spectral analysis also makes it possible to conclude that there was no breakdown instability, the threshold of which (when everything is taken into account) was not exceeded in our experiments.

For the construction of a theoretical model of the observed phenomenon the question of which of the modulation mechanisms is realized in the case under investigation is fundamental. The answer to this question was obtained by means of a direct experiment, the results of which are presented in Fig. 2. The contrast distribution shown in Fig. 2 was observed for  $\varepsilon < 0.2$ , when the cellular network has not yet filled the whole surface of the layer. It can be seen that on the periphery of the square network there is a region filled by linear bands ("rolls"), which, obviously, is a visualization of a standing wave with plane fronts. On the background of these fronts one can see contrast bands, which are arranged at right angles to the plane-wave fronts. In other words, the modulation arises as a result of an instability of the transverse type (analogous to focusing), when the corrections to the wave vectors are strictly orthogonal to the wave vectors of the original waves. The dark bands visible in Fig. 2 moved practically without noticing the boundary between the squares and the rolls. It follows from this that the presence of an orthogonal pair of waves does not hinder the onset of focusing modulation of the original standing wave. Therefore, we can expect an explanation of the observed effects in

the framework of a comparatively simple model that takes into account the excitation of only one wave pair and the modulation of the amplitudes of the waves in the direction transverse to their front. The appropriateness of this model is also confirmed by the facts that a) regimes with practically plane modulation fronts were observed (Fig. 1a), and b) the two-dimensional modulation at not-too-large supercriticalities was a superposition of regimes with one-dimensional modulation (Fig. 1b).

The results presented in Fig. 1 suggest that the dependence of the observed pattern on the bend of the boundaries of the layer is weak. Taking into account also the qualitative agreement of the results for complete and partial filling of the surface of the layer by the capillary ripple, we can conclude that reflection from the boundaries has only a weak effect on the dynamics of the wave field. This fact is explained by the absolute character of the parametric instability. The nature of the feedback that leads to the absolute instability in the given case is similar to that which obtains in the capture of parametrically excited waves by pumped pulses.<sup>9</sup> Namely, the absolute instability guarantees the observed preservation of the cells when extra walls, extraneous bodies, etc., are placed in the cuvette. The presence of the absolute instability in the medium is what makes the effect under consideration fundamentally different from the classical self-focusing of wave beams: In the present case, the modulation of the wave field has a self-oscillatory character (energy losses due to viscosity are compensated by the pumping source).

### 3. THEORETICAL MODEL

The results cited in Sec. 1 suggest the possibility of using averaged equations for the analysis of the dynamics of the wave field. Here, the principal part  $\zeta(x, y)$  of the deviation of the level of the surface is represented in the form of a sum of four waves:

$$\zeta = 1/2 [a_+ e^{ikx} + a_- e^{-ikx} + b_+ e^{iky} + b_- e^{-iky}] e^{-i\omega t} + \text{c.c.}, \quad (2)$$

where  $a_{\pm}$  and  $b_{\pm}$  are the complex amplitudes of the waves, and  $\omega = (\alpha/\rho)^{1/2} k^{3/2}$  is the capillary-wave frequency, which is assumed to be equal to  $\omega_p/2$  ( $\omega_p$  is the pumping frequency). To realize the averaging procedure we need not only conditions of the type (1) and analogous conditions on  $\partial a/\partial t$  but also the condition that the nonlinearity should be small, which, in the case of surface waves, imposes a restriction on the slope of the surface:  $|\nabla\zeta| \ll 1$ . Measurements of the slope performed using a narrow laser beam at  $\varepsilon \cong 1$  gave a value  $|\nabla\zeta| \cong 0.6$  that does not rule out the possibility of using averaged equations.

Using the expression  $\gamma = 2\nu k^2$  for the damping constant  $\gamma$  of a weak capillary wave,<sup>10</sup> we find for the relative absorption the value  $\gamma/\omega \cong 0.07 \ll 1$ . The spatial damping is characterized by the parameter  $v_g/\gamma\lambda \cong 3.4$  ( $v_g$  is the group velocity of the capillary waves). An essential role in this problem is played by the magnitude of the parameter  $\delta/\zeta_*$ , where  $\delta = (2\nu/\omega)^{1/2}$  is the thickness of the viscous boundary layer, and  $\zeta_*$  is the characteristic value of  $\zeta$ . When  $\delta/\zeta_* \gg 1$ , the boundary conditions at the surface  $z = \zeta(x, y)$

can be reduced to conditions at the unperturbed level  $z = 0$  both for the nonviscous component and for the viscous component of the velocity field of the medium in the surface wave. Because of the weak deformation of the boundary layer the nonlinear corrections to the absorption are small, but they are important at low supercriticalities.<sup>11</sup> In the limiting case of a thin boundary layer ( $\delta/\zeta_* \ll 1$ ), allowance for the damping reduces to the introduction of linear absorption with damping constant  $\gamma$  (Ref. 10) into the reduced equations for the ideal medium. For our experiment, setting  $|\nabla\zeta| \cong 2k|a|$  and  $\zeta_* \cong 4|a|$ , we obtain, at supercriticality  $\varepsilon \cong 1$ , the estimate  $\delta/\zeta_* \cong 0.22$ . Since we intend to describe the chaotic regimes at not-too-low supercriticalities, we shall use the approximation of a thin boundary layer.

For the derivation of the reduced equations we shall make use of the results of the Hamiltonian description of the nonlinear interaction of gravitational-capillary waves.<sup>12</sup> In contrast to Ref. 12, when we go over to the approximation of narrow wave packets it is necessary to retain four packets, which correspond to the two pairs of oppositely moving waves (2). In the limit of capillary waves these reduced equations take the form

$$\begin{aligned} \frac{\partial a_{\pm}}{\partial t} \pm v_g \frac{\partial a_{\pm}}{\partial x} - \frac{1}{4} i \frac{v_g}{k} \frac{\partial^2 a_{\pm}}{\partial x^2} - \frac{i}{2} \frac{v_g}{k} \frac{\partial^2 a_{\pm}}{\partial y^2} + \gamma a_{\pm} \\ = i(H + F b_+ b_-) a_{\mp}^* + i a_{\pm} [T |a_{\pm}|^2 + S |a_{\mp}|^2 + R(|b_+|^2 + |b_-|^2)], \end{aligned} \quad (3a)$$

$$\begin{aligned} \frac{\partial b_{\pm}}{\partial t} \pm v_g \frac{\partial b_{\pm}}{\partial y} - \frac{i}{4} \frac{v_g}{k} \frac{\partial^2 b_{\pm}}{\partial y^2} - \frac{i}{2} \frac{v_g}{k} \frac{\partial^2 b_{\pm}}{\partial x^2} + \gamma b_{\pm} \\ = i(H + F a_+ a_-) b_{\mp}^* + i b_{\pm} [T |b_{\pm}|^2 + S |b_{\mp}|^2 + R(|a_+|^2 + |a_-|^2)], \end{aligned} \quad (3b)$$

where

$$\begin{aligned} T = 0.0625\omega k^2, \quad S = 0.625\omega k^2, \quad R \approx -0.18\omega k^2, \\ F \approx 0.33\omega k^2, \quad H = (k/4\omega)G. \end{aligned}$$

We note that the slope of the surface, the scale of the spatial modulation, and the thickness of the viscous boundary layer in the experiments performed were such that the approximations used in the derivation of (3) were close to their limits of applicability. Taking into account also both the absence in (3) of radial nonuniformity of the pumping and difficulties with the formulation of boundary conditions at the edges of the layer, we must regard the system (3) as only a model. However, even in the framework of this model one can succeed in explaining the principal observed effects.

In the initial stage of the excitation of waves from the noise ( $|a_{\pm}| \rightarrow 0, |b_{\pm}| \rightarrow 0$ ), the system of equations (3) decomposes into two independent systems of equations for  $a_{\pm}$  and  $b_{\pm}$ . To the excitation of an elementary wave pair, propagating along the  $x$  axis, there corresponds a solution of the form  $a_{\pm}(x, t) = a_{\pm}^0(t) \exp(\pm i\Delta k x)$ , where  $\Delta k \ll k$  is the shift (from  $k$ ) of the wave number of the waves of the pair. The detuning from resonance for the frequency of each of the waves of the pair in the linear approximation is equal to  $\beta = \omega(k + \Delta k) - \omega_{p/2} \approx v_g \Delta k$ . Since the excitation of wave pairs begins when the pumping exceeds the threshold value  $H = \gamma$ , the supercriticality  $\varepsilon$  can be represented in the form

$\varepsilon = H/\gamma - 1$ . To go over to real amplitudes and phases we must set  $a_{\pm}^0 = A_{\pm} \exp(i\varphi_{\pm})$ . In the regime of stationary generation of an elementary wave pair ( $\partial/\partial t = 0$ ) the amplitudes of the waves are equal, and the phase difference  $\varphi_+ - \varphi_-$  is arbitrary. The two regimes of stationary generation are determined by the relations

$$A_{1,2}^2 = \frac{[\beta \pm (H^2 - \gamma^2)^{1/2}]}{T+S}, \quad \Phi_{1,2} = \mp (1 - \gamma^2/H^2)^{1/2}, \quad (4)$$

where  $\Phi = \varphi_+ + \varphi_-$ . Only the regime with parameters  $A_1$  and  $\Phi_1$  turns out to be stable against spatially uniform disturbances. Because the phase difference is arbitrary, it is possible that it can build up the action of the intrinsic noise of the medium. Below we shall assume that this drift of the phase proceeds substantially more slowly than the dynamical processes under consideration.<sup>4)</sup>

The excitation of one pair of waves, modulated at right angles to the front (i.e., along the  $y$  axis), is described by solutions of (3) of the form

$$a_{\pm}(x, y, t) = \tilde{a}_{\pm}(y, t) e^{\pm i\Delta h x}, \quad b_{\pm} = 0.$$

Omitting the tilde over the amplitudes  $a_{\pm}$ , we obtain for them the equations

$$\frac{\partial a_{\pm}}{\partial t} - \frac{i}{2} \frac{v_g}{k} \frac{\partial^2 a_{\pm}}{\partial y^2} + \gamma a_{\pm} = i H a_{\mp}^* - i \beta a_{\pm} + i a_{\pm} (T |a_{\pm}|^2 + S |a_{\mp}|^2). \quad (5)$$

The detuning  $\beta$  plays in (5) a fundamental role, since in the absence of dependence of  $a_{\pm}$  on  $x$  it enables us to describe frontal modulation with different wave numbers of the capillary wave. The simplest stationary ( $\partial/\partial t = 0$ ) states of the system (5) (solitons and periodic beats) were found in Ref. 13. However, in Ref. 13 it was proved that these states are unstable "in the small", and so we cannot invoke them to explain the experiments described in Sec. 1.

We shall show that the problem of the one-dimensional modulation of the square cells can also be reduced to the solution of a system of the form (5). We make in (3) the replacement<sup>5)</sup>

$$a_{\pm} = \tilde{a}_{\pm}(y) e^{\pm i\Delta h x}, \quad b_{\pm} = \tilde{b}_{\pm}(y) e^{\pm i\Delta h x}.$$

Considering the distributions  $\tilde{a}_{\pm}(y)$  and  $\tilde{b}_{\pm}(y)$ , which oscillate repeatedly over the length  $l_2$  of the system, we introduce the operation:  $\langle \dots \rangle = 1/l_2 \int_0^{l_2} (\dots) dy$ , application of which makes it possible to eliminate derivatives with respect to  $y$  from the equation for  $\tilde{a}_{\pm}$  and  $\tilde{b}_{\pm}$ . Since the operator  $v_g \partial/\partial y$  appearing in the equation for  $\tilde{b}_{\pm}$  is considerably more sensitive than the operator  $(v_g/2k) \partial^2/\partial y^2$  to the small width of the wave packet, the deviations  $b'_{\pm} = \tilde{b}_{\pm} - \langle \tilde{b}_{\pm} \rangle$  of  $\tilde{b}_{\pm}$  from its average value turn out to be small. In fact, taking into account the condition  $|b'_{\pm}| \ll |\langle \tilde{b}_{\pm} \rangle|$ , we obtain for  $b'_{\pm}$  an equation of the form

$$v_g \partial b'_{\pm} / \partial y = \pm i \langle \tilde{b}_{\pm} \rangle R (|a_+|^2 + |a_-|^2), \quad (6)$$

where  $|a_{\pm}|^2 = |\tilde{a}_{\pm}|^2 - \langle |\tilde{a}_{\pm}|^2 \rangle$ . Application of the averaging operation to the system of equations for  $\tilde{a}_{\pm}$  and  $\tilde{b}_{\pm}$  makes it possible to relate  $\langle \tilde{b}_{\pm} \rangle$  to the average  $\langle \tilde{a}_{\pm} \rangle$  and to

averages of nonlinear combinations of  $\tilde{a}_{\pm}$ . For the amplitudes  $\tilde{a}_{\pm}$  themselves we obtain a system of equations of the form (5), but with different values of the detuning and pumping:

$$\beta \rightarrow \beta + R (|\langle \tilde{b}_+ \rangle|^2 + |\langle \tilde{b}_- \rangle|^2), \quad H \rightarrow H + F \langle b_+ \rangle \langle b_- \rangle.$$

Denoting the scale of the modulation along  $y$  by  $\Lambda_y$  and assuming that  $|a_{\pm}|$ ,  $\langle b_{\pm} \rangle$ , and  $(|a_{\pm}|^2)^{1/2}$  are quantities of the same order, we obtain the estimates

$$\frac{v_g}{2k} \frac{|a|}{\Lambda_y^2} \sim (S+T) |a|^3, \quad v_g \frac{|b'|}{\Lambda_y} \sim R |a|^3.$$

Then for a narrow wave packet ( $k\Lambda_y \gg 1$ ) we obtain from (6) the estimate

$$|b'| \sim \frac{R}{S+T} \frac{|a|}{k\Lambda_y} \ll |a|.$$

Thus, within the limits of applicability of the system (3) there exists an analogy between the processes of the one-dimensional modulation of the square cells and the transverse modulation of the rolls.

Before moving on to study the system (5), we shall discuss the question of the existence of uniform (in the direction of propagation) regimes in a bounded system. In the case of one wave pair, distributions that are nonuniform in  $x$  are described by the system of equations

$$\frac{\partial a_{\pm}}{\partial t} \pm v_g \frac{\partial a_{\pm}}{\partial x} + \gamma a_{\pm} = i H a_{\mp}^* + i a_{\pm} (T |a_{\pm}|^2 + S |a_{\mp}|^2). \quad (7)$$

We shall consider first the stationary solutions of (7) in the case of complete absence of reflection of waves from the boundary:  $a_+ = 0$  at  $x = 0$  and  $a_- = 0$  at  $x = l_1$ . Going over to real amplitudes and phases, we obtain the equations

$$v_g dA_+/dx = HA_- \sin \Phi - \gamma A_+, \quad v_g dA_-/dx = -HA_+ \sin \Phi + \gamma A_-. \quad (8)$$

In addition, the stationary problem has an integral of the form

$$A_+ A_- \cos \Phi + (T-S) A_+^2 A_-^2 / 2H = C = \text{const}. \quad (9)$$

For complete absence of reflection at the edges,  $C = 0$ . As a result, the systems (8) and (9) are transformed to the form

$$v_g dA_+/dx = \pm HA_- (1 - r^2 A_+^2 A_-^2)^{1/2} - \gamma A_+, \quad (10)$$

$$v_g dA_-/dx = \mp HA_+ (1 - r^2 A_+^2 A_-^2)^{1/2} + \gamma A_-,$$

where  $r = (T-S)/2H$ . The equations (10) have the integral

$$A_+^2 + A_-^2 = \pm (2\gamma/rH) \arcsin(rA_+A_-) + \text{const}$$

and can be integrated in quadratures. However, a qualitative investigation of them appears to be more visualizable. The phase space of (10) is two-sheeted, and the splicing of the sheets corresponding to the different signs in (10) is along the hyperbolas  $|A_+A_-| = r$ . The phase plane for the system (10) with the first sign in front of the square root is shown in Fig. 3. The phase portrait of the second sheet is the mirror image, about the axis  $A_-$ , of the phase portrait shown in Fig. 3. The trajectories corresponding to the solution of the sta-

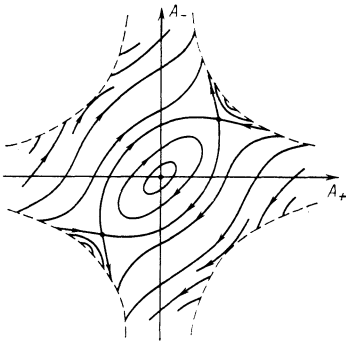


FIG. 3. Phase portrait of the system (10).

tionary boundary-value problem pass from the line  $A_+ = 0$  to the line  $A_- = 0$  over an interval in  $x$  equal to the length  $l_1$  of the system. If the length of the system is considerably greater than one-quarter of a period of revolution about center, i.e., if  $l_1 \gg 1/2\pi v_g (H^2 - \gamma^2)^{-1/2}$ , the phase trajectory corresponding to the simplest (principal) mode of stationary generation passes near the saddle-point separatrix. At not-too-low supercriticality this condition is fulfilled in the experiments (Sec. 1), since many scales of linear damping of waves are accommodated over the length of the system:  $\gamma l_1 / v_g \gg 1$ . The distribution of amplitudes in the principal mode for  $\gamma l_1 / v_g = 10$  and  $\varepsilon = 1$  is shown in Fig. 4. The fact that the phase trajectory stays near the saddle point for a long time implies that in the larger part of the layer the field is close to being a uniform standing wave:

$$A_+ = A_- = [2/(T-S)]^{1/2} (H^2 - \gamma^2)^{1/4}. \quad (11)$$

In this region the wave number of the capillary wave acquires a correction  $\Delta k = \pm v_g d\varphi_{\pm} / dx \cong \text{const}$ , to which corresponds the frequency detuning

$$\beta = [(S+3T)/(S-T)] (H^2 - \gamma^2)^{1/2} \approx 1.44 (H^2 - \gamma^2)^{1/2}. \quad (11)$$

In a long layer there is a finite number of stationary-generation modes, to which correspond phase trajectories executing one or more revolutions about the center. To answer the question of the stability of the different stationary regimes we integrated the partial differential equations (7) numerically.<sup>6)</sup> It was found that, even in the case of initial sources oscillating rapidly in space, a distribution in the form of the principal mode is established (Fig. 4). Thus, in a long layer

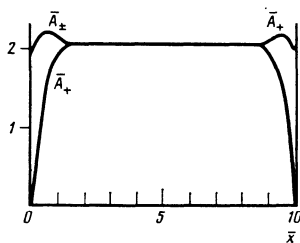


FIG. 4. Structure of the stationary-generation field, corresponding to the principal mode in the complete absence of reflection from the boundaries of the layer ( $A_{\pm} = A_{\pm} [(T+S)/\gamma]^{1/2}$ ,  $\bar{x} = \gamma x / v_g$ ).

there is a tendency toward the formation of a distribution which is uniform over the larger part of the length of the layer and to which corresponds a definite value of the frequency detuning  $\beta$ . The "roughness" of this state makes it possible to disregard in (7) the dispersion for the envelope curves.

We note that an analogous analysis (with allowance for finite reflection from the boundaries) gives a value of  $\beta$  which, depending on the sign of the constant  $C$  in (9), can differ from (11) in either direction.<sup>7)</sup> In addition, as shown by the numerical integration of (7), from a given initial disturbance a profile of the type shown in Fig. 4 is rapidly formed, with a uniform central part within which the expressions (4) are valid. However, the value of  $\beta$  within the uniform region was smaller by a factor of 2–2.5 than that given, and reached the level (11) only after a long time ( $\gamma t \sim 200$ –300). Finally, in the presence of modulation of  $a_{\pm}$  along the transverse coordinate  $y$ , we can expect other effective values of  $\beta$ , since the stability condition should now be satisfied by an  $a_{\pm}$  profile with modulation along  $y$ . For the reasons enumerated, in the investigation of the steady-state regimes of focused modulation in the framework of the one-dimensional model (Eqs. (5) the value of the detuning  $\beta$  remains an undetermined parameter. In choosing it we must be guided by comparison with the results of experiment, regarding (11) only as an estimate of the quantity  $\beta$ .

#### 4. THE FOCUSING INSTABILITY. THE ONSET AND DEVELOPMENT OF SPATIOTEMPORAL CHAOS

Confining ourselves to an investigation of the modulation of standing waves, in (5) we set  $a_{\pm} = a(y, t) \times \exp(\pm \frac{1}{2} i \varphi_0)$ , where  $\varphi_0$  is the constant phase difference of the waves in the pair. After changing to dimensionless variables  $u = a[(S+T)/\gamma]^{1/2}$ ,  $\eta = y(v_g/2\gamma k)^{-1/2}$ , and  $\tau = \gamma t$ , we obtain the following equation for  $u$ :

$$\partial u / \partial \tau - i \partial^2 u / \partial \eta^2 + u = i h u^* + i u |u|^2 - i \sigma u, \quad (12)$$

where  $\sigma = \beta / \gamma$  and  $h = H / \gamma$  are the dimensionless detuning and pumping parameters. Because of the phenomenon of synchronization of the phases of wave pairs (see below), passing from (5) to one equation does not lead to loss of generality when we are considering steady-state processes.<sup>8)</sup>

Equation (12), which contains the dependence of the energy source on the phase of the field, may be called the parametric analog of the Ginzburg-Landau equation. To investigate the instability of the stationary uniform state  $u = u_0$  we set  $u = u_0 + \psi$  and make use of Eq. (12) linearized with respect to  $\psi$ :

$$\partial \psi / \partial \tau - i \partial^2 \psi / \partial \eta^2 + (1 + i \sigma - 2i |u_0|^2) \psi = i (h + u_0^2) \psi^*. \quad (13)$$

For  $u_0$  we use the value of the field in the stable (against uniform perturbations) stationary state [see the expressions (4) for  $A_1$  and  $\Phi_1$ ]. Substitution into (13) of the solution in the form

$$\psi = C_1 e^{i k y - i \Omega \tau} + C_2 e^{-i k y + i \Omega^* \tau}$$

( $C_{1,2} = \text{const}$ ) leads to the following expression for the

modulation frequency:

$$\Omega = -i \pm \{ [\kappa^2 - \sigma - 2(h^2 - 1)^{1/2}]^2 - (\sigma^2 + 1) \}^{1/2}. \quad (13')$$

For  $\sigma > 0$ , instability arises in the interval

$$2^{1/2} (h^2 - 1)^{1/4} < |\kappa| < 2^{1/2} [\sigma + (h^2 - 1)^{1/2}]^{1/2};$$

for  $-(h^2 - 1)^{1/2} < \sigma < 0$  the boundaries of this interval are exchanged. The maximum growth constant is reached at  $|\kappa_m| = [\sigma + 2(h^2 - 1)^{1/2}]^{1/2}$  and is equal to  $(\text{Im } \Omega)_{\text{max}} = (\sigma^2 + 1)^{1/2} - 1$ . With decrease of  $\sigma$  the value of  $|\kappa_m|$  decreases monotonically, and at the boundary of the existence of the stationary regime ( $\sigma = -(h^2 - 1)^{1/2}$ ) becomes equal to  $|\kappa_m| = (h^2 - 1)^{1/4}$ . If we assume that the period of the steady-state modulation is determined by the most rapidly growing disturbance, the characteristic period of the modulation along  $y$  should not exceed the quantity

$$\Lambda_{\text{max}} = \lambda (h^2 - 1)^{-1/4} (\pi v_g / \gamma \lambda)^{1/2}.$$

For the conditions of the experiments described in Sec. 1, at supercriticality  $\varepsilon = 0.2$  we obtain  $\Lambda_{\text{max}} \cong 4\lambda$ , and at  $\varepsilon = 1$  we have  $\Lambda_{\text{max}} \cong 2.4\lambda$ . These estimates agree well with the fact that in the experiment modulation with periods greater than  $4\lambda$  was practically not observed.

To investigate the steady-state regimes of focused modulation we integrated Eq. (12) numerically. After introduction of the variable  $n = \eta Q^{-1/2}$  ( $Q = \text{const}$ ) and replacement of  $\partial^2 / \partial n^2$  by the second difference, Eq. (12) goes over into the discrete analog of the parametric Ginzburg-Landau equation (in analogy with Ref. 15):

$$\partial u_n / \partial \tau - iQ(u_{n+1} + u_{n-1} - 2u_n) + u_n = ihu_n^* + iu_n |u_n|^2 - i\sigma u_n. \quad (14)$$

If we introduce the parameter  $p$ , equal to the number of discretization steps in the wavelength  $\lambda$  of the capillary wave, we obtain  $Q = (v_g / \gamma \lambda) p^2 / 4\pi$ .

The system (14) replaces the active medium by a chain of coupled parametric generators, each of which is equivalent to an elementary block of the medium, with length  $\lambda / p$ . The coupling between the generators vanishes in spatially

uniform oscillations of the chain (in which  $u_n$  does not depend on  $n$ ). The indicated analogy makes it possible to introduce an element of physical modeling into the numerical solution of (13). However, it should be remembered that the representation (14) approximates to the original partial differential equation only when  $\text{Re } u_n$  and  $\text{Im } u_n$  change little over one link of the chain (the coupling builds up smoothly). Another, not unimportant advantage of using (14) rather than the formal network procedures is that the original partial differential equation reduces to a finite-dimensional dynamical system. This makes it possible to use for the analysis the well-developed apparatus of the theory of dynamical systems.

The system of equations (14), written for  $\text{Re } u_n$  and  $\text{Im } u_n$ , was solved on a computer. The calculations were performed for the case with  $N = 175$  links and  $Q = 10$ . In this case,  $p \cong 6.1$ , i.e., the condition that the field vary little over one link coincides with the condition for applicability of the original equations (1), and the length of the layer is equal to  $N/p \cong 30$  wavelengths of the capillary wave. The boundary conditions at the ends of the chain were specified in the form  $u_0 = u_1$  and  $u_{N+1} = u_N$ , which, for the distributed model, coincides with the free-ends conditions ( $\partial u / \partial y = 0$  at the edges of the layer). To realize the different modulation regimes we specified initial conditions of two types: 1) small deviations on the background of the uniform equilibrium state  $u_0$ , and 2) large-amplitude distributions  $u_n$ , oscillating rapidly along the chain. We studied the steady-state modulation regimes that arise upon increase of  $h$  (the degree of nonequilibrium of the system). Here, in accordance with the considerations presented in Sec. 2, we chose the law of variation of the detuning in the form  $\sigma = (h^2 - 1)^{1/2}$ . We also carried out sampling integration of (14) with other values of  $\sigma$ .

At low supercriticalities, complicated stationary states with a large number of oscillations on the  $|u_n|$  profile arose in the chain (Fig. 5). In the case of initial conditions of the type 1), the emergence into the stationary regime occurred via a secondary instability, with periodic spatial modulation

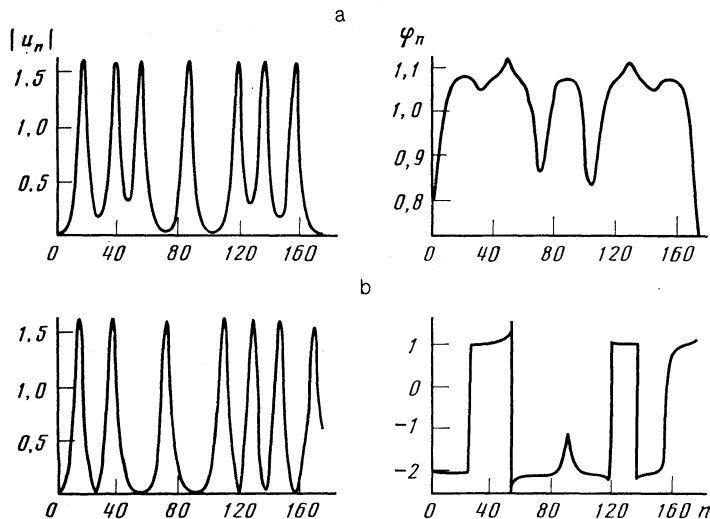


FIG. 5. Examples of stationary amplitude and phase distributions established with the same parameter values ( $\varepsilon = 0.2$ ,  $\beta = 0.66$ ) but different initial conditions: a) in the form of smooth small deviations from the regime of uniform generation; b) in the form of intense disturbances oscillating rapidly along the chain.

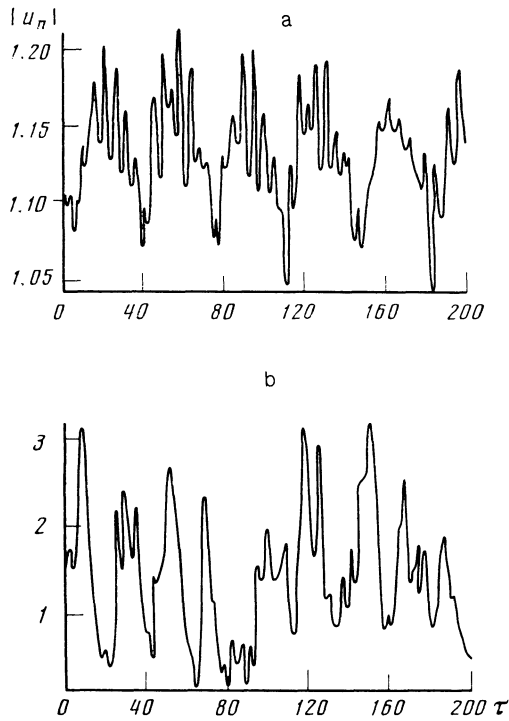


FIG. 6. Steady-state oscillations of the amplitude of the field  $u_n$  at the center of the chain: a) near the threshold for the onset of chaos ( $\varepsilon = 0.85$ ,  $\beta = 1.58$ ); b) for developed chaos ( $\varepsilon = 1.2$ ,  $\beta = 1.92$ ).

associated with the development of the focused instability. The phase  $\varphi_n = \arg u_n$  oscillated relatively weakly along the chain (Fig. 5a). Stationary regimes of another type were obtained with the initial conditions 2). Their structure resembled the product of a complex function, rapidly oscillating in modulus and with relatively small changes of phase, with a real alternating function. Correspondingly, at the nodes of the amplitude profile the phase of the field changed by approximately  $\pi$  (Fig. 5b). With increase of  $h$  the troughs between the beats on the  $|u_n|$  profile contracted. At a value  $h \cong 1.85$  the stationary state became unstable—weak oscillations of  $|u_n|$  in time appeared (Fig. 6a). The character of the

oscillations indicates the realization of a transition to chaos via intermittency.<sup>16</sup> The results obtained by solving (14) for the developed chaotic regime ( $h = 2.2$ ) are presented in Fig. 7. The spatial distributions of  $|u_n|$  and  $\varphi_n$  retained properties characteristic of the stationary regimes. For example, for the initial conditions 2) groups of peaks of  $|u_n|$  appeared, separated by nodes to which corresponded discontinuous changes of phase by  $\pi$  (Fig. 7a). The change of the spatial structure of  $|u_n|$  in the steady-state regime included the following elements: 1) rapid (with characteristic time  $\tau_1 \sim 4$ ) processes of growth or decay of the amplitudes of the peaks, shift of the peaks through a distance of the order of their width, and the appearance or disappearance of peaks within a group bounded by nodes on the  $|u_n|$  profile; 2) substantial drops in the amplitude  $|u_n|$  over one link in a time  $\tau_2 \sim 20$ ; 3) a slow drift of the points of discontinuous phase change by  $\pi$  (and of the nodes on the  $|u_n|$  profile) with characteristic time  $\tau_3 \sim 200-300$ . The times  $\tau_1$  and  $\tau_2$  can be seen clearly on the realization shown in Fig. 6b. Depending on the intensity of the initial source, spatial distributions with different numbers of discontinuous phase changes by  $\pi$  arose, but after a number of coalescences of phase-discontinuity points a regime with a constant number of such points, executing a slow random walk, was established. Limiting regimes with different numbers of phase-discontinuity points were obtained, indicating the presence of several stochastic attracting sets (strange attractors) in the phase space of the system (14). The fact that the limit set is stochastic was verified by a calculation of the first Lyapounov exponent of a trajectory on the attractor<sup>17</sup>:

$$\lambda_1 = \frac{d}{d\tau} \ln [\overline{l(\tau)/l(0)}],$$

where the bar denotes a time average, and

$$l(\tau) = \left[ \sum_{n=1}^N (\text{Im } u_n^{(1)} - \text{Im } u_n^{(2)})^2 + \sum_{n=1}^N (\text{Re } u_n^{(1)} - \text{Re } u_n^{(2)})^2 \right]^{1/2}$$

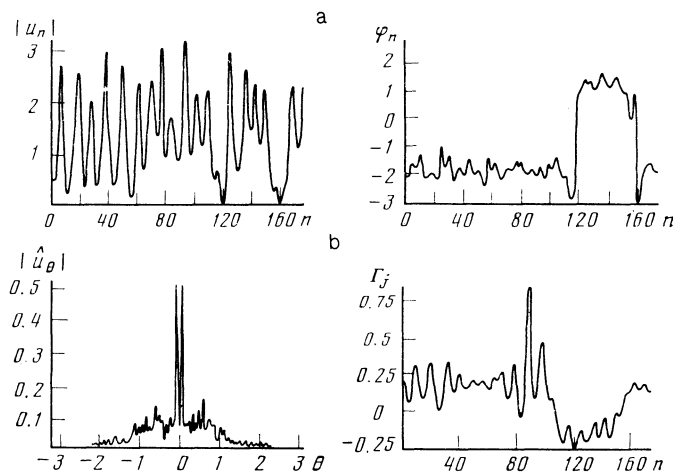


FIG. 7. Characteristics of developed spatiotemporal chaos for  $\varepsilon = 1.2$  and  $\beta = 1.92$ : a) instantaneous distributions of the amplitude and phase; b) spatial spectrum and cross correlation function ( $\theta$  is the phase shift per link of the chain).

is the distance in the phase space of (14) between two infinitesimally close realizations determined by integration of the linearized system (14). For the regime shown in Fig. 7, for averaging times  $\tau > 30$ , it was found that  $\lambda_1$  approaches a constant value  $\lambda_1 \cong 0.273$ .

Figure 7b shows the spatial spectrum of  $u_n$  and the (spatial) cross correlation function about the center of the chain:

$$\Gamma_j = \text{Re}(\overline{u_{88}u_j'} - \overline{u_{88}u_j}^*).$$

The modulation of the average (over the period of the spatial oscillations) gives discrete peaks in the long-wavelength region of the spatial spectrum (the zeroth harmonic has been discarded in Fig. 7b). It can also be seen that the correlation of the random pulsations along the chain decreases significantly over a distance of the order of the width of a peak.

In the case of initial conditions of the type 1), discontinuous changes of phase by  $\pi$  were absent and the spatial spectrum of the modulation did not contain sharply pronounced long-wavelength peaks. The temporal changes contained all the elements that appeared in the regimes that arise under initial conditions of the type 2). In contrast to Fig. 7b, the time correlation function did not have in the negative region a spike associated with a discontinuous change of phase by  $\pi$ .

Integration of the system (14) for  $h = 2.2$  and detunings  $\sigma > 0$  showed that there exists a threshold detuning  $\sigma \cong 2.4$ , above which the regimes described above are destroyed: Almost stationary distributions in the form of small peaks of  $|u|$ , separated by deep troughs with  $|u| \rightarrow 0$ , appear. In this region of detunings lies the value  $\beta \cong 2.83$  determined by (11).

With the aim of ascertaining the possibility of going over from the system (5) to the homogeneous equation (12) we integrated (5) numerically, using the scheme described above. To explain the results of the calculation it is useful to change in (5) from the real amplitudes  $A_{\pm}$  and phases  $\varphi_{\pm}$  to the variables

$$A_{s,d} = (A_+ \pm A_-)/2, \quad \varphi_{s,d} = (\varphi_+ \pm \varphi_-)/2.$$

When  $A_d = 0$  and  $\varphi_d = 0$ , the system of equations for  $A_s$  and  $\varphi_s$  is equivalent to Eq. (12). The difference between them will be small when the difference in the amplitudes is small ( $A_d \ll A_s$ ) and the derivatives of the phase difference  $\varphi_d$  with respect to  $t$  and  $y$  are small. Thus, it is sufficient to detect synchronization of rapid changes of the phases  $\varphi_{\pm}$  in space and in time. Precisely such synchronization was observed in the numerical solution.<sup>9)</sup>

The pattern obtained above for the chaotic dynamics of the modulation peaks is in good qualitative accord with the results of the experiments. The results of the calculation for low supercriticalities predict the formation of large troughs on the modulation profile, and these can be observed in the experiments (see Fig. 2). The earlier (at  $h < 1.85$ ) appearance of nonstationary modulation in the experiment can be attributed to the two-dimensional character of the real modulation, i.e., to the not entirely suitable choice of dependence of  $\sigma$  on  $h$ . In addition, the drift times of the dark bands are in agreement with the rearrangement times in the establish-

ment of the stationary states in the numerical calculation. For example, for  $h = 1.4$  ( $\varepsilon = 0.4$ ) these are times  $t \sim 100\gamma^{-1} \sim 3$  sec. The proposed model makes it possible to explain the establishment of a developed chaotic regime whose elements are in good qualitative agreement with the pattern of rearrangements that is observed experimentally (see Sec. 1). In real time the fastest rearrangements for  $h = 2.2$  have a timescale  $t_2 \cong \tau_2\gamma^{-1} \sim 0.12$  sec, which agrees with visual estimates for the regime of developed chaos.

## 5. CONCLUSION

The presently investigated onset of parametric turbulence of capillary waves is an example of the creation, in a real nonequilibrium medium, of spatiotemporal chaos that is dynamical in nature and does not require for its explanation any prior hypotheses or assumptions. The transition to chaos and its finite-dimensional description are determined by the resonance character of the parametric excitation of waves and do not depend on the boundary conditions on the periphery of the medium.

To describe the turbulence, we have derived here a parametric variant of the well-known Ginzburg-Landau equation—a variant that is evidently just as universal for parametric media as its analog for, say, thermal convection or surface waves excited by wind, in cases when the instability threshold is slightly exceeded.

We shall stress here two further circumstances. The experimentally observed two-dimensional chaos on a background of elementary cells near the threshold for the onset of turbulence is almost a superposition of one-dimensional mutually orthogonal structures with random modulation, and it is this which justifies the construction of a one-dimensional theory on the basis of Eq. (12). As the numerical experiments have shown, Eq. (12) with the same parameter values can describe different steady state chaotic regimes. This implies that in its phase space several different stochastic attractors exist simultaneously, and which one of these is eventually reached is determined by the initial conditions. Visually, in the experiment, a set of spatial forms (structures), established on the background of the capillary ripple at the same supercriticality, corresponds to this set of attractors.

<sup>1)</sup>The amplitude profile of the vibrations had at the center of the cuvette a weakly expressed maximum.

<sup>2)</sup>It can be shown that as soon as the size of the pumping region becomes greater than 1 cm the value of the threshold practically coincides with the threshold for uniform excitation.

<sup>3)</sup>The appearance of the modulation is not due to nonstationarity of the amplitude and phase of the pumping, since the relative width of the pumping spectrum did not exceed  $10^{-5}$ .

<sup>4)</sup>Application of the  $S$ -theory to one wave pair requires that the opposite condition be fulfilled.<sup>2</sup>

<sup>5)</sup>The results can also be generalized to the case when  $\bar{a}_{\pm}$  and  $\bar{b}_{\pm}$  depend on  $t$ .

<sup>6)</sup>After introduction of the dimensionless variables  $\bar{a}_{\pm} = a_{\pm} [(S+T)/\gamma]^{1/2}$ ,  $\tau = \gamma t$ , and  $\bar{x} = \gamma x/v_g$ , only the one parameter  $T/S = 10$  remains in the equations.

<sup>7)</sup>The quantity  $C$  in this case is found from the condition that the total advance of the phase along the resonator be a multiple of  $2\pi$ .

<sup>8)</sup>The problem of the longitudinal modulation in the parametric excitation of  $\pi$ -oscillations in periodic structures leads to an analogous equation.<sup>14</sup>

<sup>9)</sup>Only very smooth changes of  $\varphi_d$  along the chain (changes with a length scale of the order of the length of the layer) were found to be relatively long-lived.

- <sup>1</sup>Yu. M. Aliev and E. Ferlengi, Zh. Eksp. Teor. Fiz. **57**, 1623 (1969) [Sov. Phys. JETP **30**, 877 (1970)].
- <sup>2</sup>V. E. Zakharov, V. S. L'vov, and S. S. Starobinets, Usp. Fiz. Nauk **114**, 609 (1974) [Sov. Phys. Usp. **17**, 896 (1975)].
- <sup>3</sup>V. A. Briskman and T. F. Shaïdurov, Dokl. Akad. Nauk SSSR **180**, 1315 (1968) [Sov. Phys. Dokl. **13**, 540 (1968)].
- <sup>4</sup>V. G. Bashtovoi and Yu. D. Barkov, Magn. Gidrodin. **16**, No. 4, 6 (1980) [Magnetohydrodynamics (USSR) **16**, 335 (1980)].
- <sup>5</sup>M. D. Gabovich and V. Ya Poritskiï, Zh. Eksp. Teor. Fiz. **85**, 146 (1983) [Sov. Phys. JETP **58**, 86 (1983)].
- <sup>6</sup>V. G. Nevolin, Inzh.-Fiz. Zh. **47**, 1028 (1984) [J. Eng. Phys. (USSR) **47** (1984)].
- <sup>7</sup>A. B. Ezerskiï, P. I. Korotin, and M. I. Rabinovich, Pis'ma Zh. Eksp. Teor. Fiz. **41**, 129 (1985) [JETP Lett. **41**, 157 (1985)].
- <sup>8</sup>L. D. Rozenberg (ed.), Fizika i tekhnika moshchnogo ul'trazvuka (Physics and Technology of High-intensity Ultrasound), Vol. 3, Nauka, Moscow (1970) [English translation (High Intensity Ultrasonic Fields) published by Pleunum Press, New York (1971)].
- <sup>9</sup>A. P. Sukhorukov and A. K. Shchednova, Zh. Eksp. Teor. Fiz. **60**, 1251 (1971) [Sov. Phys. JETP **33**, 677 (1971)].
- <sup>10</sup>O. M. Phillips, *The Dynamics of the Upper Ocean*, Cambridge University Press (1977) [Russ. transl., Gidrometeoizdat, Leningrad (1980)].
- <sup>11</sup>D. V. Lyubimov and A. A. Cherepanov, Nekotorye zadachi ustoiçhivosti poverkhnosti zhidkosti (Certain Problems of the Stability of a Liquid Surface), Preprint, Ural Scientific Centre, Academy of Sciences of the USSR, Sverdlovsk (1984).
- <sup>12</sup>V. E. Zakharov, Zh. Prikl. Mekh. Tekh. Fiz., No. 2, 89 (1968) [J. Appl. Mech. Tech. Phys. (USSR)].
- <sup>13</sup>V. S. L'vov, A. M. Rubenchik, V. V. Sobolev, and V. S. Synakh, Fiz. Tverd. Tela **15**, 793 (1973) [Sov. Phys. Solid State **15**, 550 (1973)].
- <sup>14</sup>A. B. Ezerskiï, M. I. Rabinovich, Yu. A. Stepanyants, and M. F. Shapiro, Zh. Eksp. Teor. Fiz. **76**, 991 (1979) [Sov. Phys. JETP **49**, 500 (1979)].
- <sup>15</sup>A. V. Gaponov-Grekhov, M. I. Rabinovich, and I. M. Starobinets, Dokl. Akad. Nauk SSSR **279**, 596 (1984) [Sov. Phys. Dokl. **29**, 914 (1984)].
- <sup>16</sup>Y. Pomeau and P. Manneville, Commun. Math. Phys. **74**, 189 (1980).
- <sup>17</sup>J.-P. Eckmann and D. Ruelle, Rev. Mod. Phys. **57**, 617 (1985).

Translated by P. J. Shepherd